Modeling of 3-dimensional objects by subdivision schemes

Ghulam Mustafa[1], Mehwish Bari[2], Sidra Nosheen[3]
The Islamia University of Bahawalpur
Pakistan
ghulam.mustafa@iub.edu.pk[1], mehwishbari@yahoo.com[2], ssbajwa786@gmail.com[3]

ABSTRACT: *In this paper, we model the different objects with the help of one of the optimize subdivision algorithm. First, least squares method has been used to fit bivariate cubic polynomial to the $(2n+1)^2$-observations. Then from this polynomial the construction of $(2n + 1)^2$-point approximating subdivision schemes are presented for $n \geq 2$. The proposed schemes can be used for the modeling of different objects in three dimensional spaces. Applications and visual performances of the proposed schemes have also been presented to show the performance of proposed work.*

Keywords: Polynomial observations, Subdivision algorithm, Object modeling, 3-dimensional objects

Received: 12 June 2016, Revised 10 July 2016, Accepted 19 July 2016

1. Introduction

The method of least squares is one of the golden techniques in statistics. In 1805, Frenchman Legendre and American Adrian in 1808 independently presented the idea about least squares analysis. The least squares method is identified by an equation with certain parameters to observed data and to estimate these statistical properties of the data. In Figure 1, the solid line displays the curve formed by least squares method. One can see that the solid line does not consistent with the initial sample/ polyon (doted line). Therefore, an alternative technique to represent data is required.

The most important, significant and emerging modeling tool in computational science, computer applications, computer aided geometric design, engineering, space science, medical image processing and scientific visualization is subdivision. Subdivision is a process of generating curves and surfaces as a limit of sequence of successively refined control polygons. By this technique, at each refinement level, the new injected points on a improved grid are calculated by affine combination

of previously existing points. In the limit of the recursive procedure, data is defined on a dense set of points. The objective of subdivision schemes is to make a smooth and visually nice limit curve or surface whose shape is controlled by primary data. Their foremost benefit is the ease with which they accommodate the construction of smooth surfaces in the arbitrary topology setting. They also offer many favorable computational properties for applications ranging from surface compression to physical modeling.

Figure 1. Dots show the initial polygon where as solid line shows the curve formed by least square method

A subdivision surface, in the field of 3D computer graphics, is a method of representing a smooth surface through the specification of a thicker piecewise linear polygon mesh. The smooth surface can be calculated from the coarse mesh as the limit of a recursive process of subdividing each polygonal characteristic into smaller faces that better approximate the smooth surface.

Chaikin [2] extended the algorithm to generate 3D curves with techniques for their application to surface representation. Doo and Sabin [3] extended the Chaikin algorithm to subdivision surfaces and could be applied to control meshes of arbitrary topology. Conti and Romani [4] presented an algebraic perspective of the de Rham transform of a binary subdivision scheme and propose well-designed approach for constructing dual m-ary approximating subdivision schemes of de Rham-type. Antonelli et al. [5] discussed two main problems which limited the usage of subdivision surfaces in computer-aided design (CAD) systems and concerned the integration into the modeling work flows. They proposed integration of subdivision surfaces in a CAD system and also introduced new CAD system paradigm with an extensible geometric kernel.

Kosinka et al. [6] discussed univariate and bivariate binary subdivision schemes based on cubic B-splines through double knots and also analyzed bivariate cubic schemes through double knots at extraordinary points. Beccari et al. [7] defined non tensor product subdivision schemes interpolating regular grids of control points and generated limit surfaces with a better behavior than the well-established tensor product subdivision and spline surfaces. Least squares progressive and iterative approximation (LSPIA) constructs a series of fitting curves/surfaces by adjusting the control points iteratively, and the limit curve/surface. Deng and Lin [8] developed progressive and iterative approximation for least squares fitting. Shi and Liang [9] presented a novel integration method that can fuse registered partially overlapping multi-view range images into a single-layer, smooth and detailed point set surface. Vilca et al. [10] proposed and discussed a bivariate Birnbaum- Saunders regression model and its properties. These method was efficient only overlapping points were processed and the non-overlapping points are remained as they were.

Dyn et al. [11] firstly introduced and analyzed univariate, linear, and stationary subdivision schemes for refining noisy data by fitting local least squares polynomials. They also discussed their convergence, smoothness, basic limit functions and several numerical experiments that demonstrate the limit functions generated by these schemes from initial noisy data. Mustafa et al. [12] introduced the l_1-regression based subdivision schemes with fast numerical optimization method which properly handle noisy data with impulsive noises and outliers. They also extended the least squares regression based subdivision schemes from the fitting of a curve to the set of observations in 2-dimensional space to a p-dimensional hyperplane to a set of point observations in (p+1)-dimensional space. In this paper, we extended Dyn et al. (2015) and Mustafa et al. (2015) work by fitting bivariate cubic polynomial to the $(2n + 1)^2$-observations.

2. Non-Tensor Product Scheme Based On Bivariate Cubic Polynomial

We first fit the bivariate cubic polynomial to the $(2n+1)^2$- observations/data by using the least squares method. Then we drive the $(2n + 1)^2$-point approximating subdivision scheme.
Let

$$f(x, y) = \beta_1 + \beta_2 x + \beta_3 y + \beta_4 x^2 + \beta_5 xy + \beta_6 y^2 + \beta_7 x^3 + \beta_8 x^2 y + \beta_9 xy^2 + \beta_{10} y^3, \quad (1)$$

be the bivariate cubic polynomial to be fitted of the data $x = r, y = s, -n \leq r, s \leq n, n \geq 2$. So a general bivariate polynomial function of degree three with respect to the observations ($x = r, y = s, f_{r,s}$) can be written as

$$f_{r,s} \approx f(r,s) = \beta_1 + \beta_2 r + \beta_3 s + \beta_4 r^2 + \beta_5 rs + \beta_6 s^2 + \beta_7 r^3 + \beta_8 r^2 s + \beta_9 rs^2 + \beta_{10} s^3.$$

Since the method of least squares calls for the selection of polynomial that minimizes *R*, the sum of the squares of differences between observed value *f*(*r*, *s*) and the corresponding exact value $f_{r,s}$. So by differentiating

$$R = \sum_{r=-n}^{n} \sum_{s=-n}^{n} [f_{r,s} - (\beta_1 + \beta_2 r + \beta_3 s + \beta_4 r^2 + \beta_5 rs + \beta_6 s^2 + \beta_7 r^3 + \beta_8 r^2 s + \beta_9 rs^2 + \beta_{10} s^3]^2,$$

with respect to $\beta_1, \beta_2, \ldots, \beta_{10}$ and then setting them to 0, we get the ten normal equations. After solving and simplifying those equations, we get the values of Beta's. By substituting the values of $\beta_1, \beta_2, \ldots, \beta_{10}$ in equation (1) and after simplifying, we get,

$$f(x,y) = \frac{1}{\varpi}\left[\sum_{r=-n}^{n}\left\{\sum_{s=-n}^{n}(\beta_1 + \beta_2 x + \beta_3 y + \beta_4 x^2 + \beta_5 xy + \beta_6 y^2 + \beta_7 x^3 + \beta_8 x^2 y + \beta_9 xy^2 + \beta_{10} y^3) f_{r,s}\}\right\},\right]$$

$$\beta_1 = (n-1)(n+2)n^2(n+1)^2(14n^2 + 14n - 15r^2 - 15s^2 - 3),$$

$$\beta_2 = 5rn(n+1)\{18n^4 + 36n^3 - (9s^2 + 21r^2 + 3)n^2 - (21r^2 + 9s^2 + 21)n + 7r^2 + 18s^2 + 5\},$$

$$\beta_4 = -15n(n^2 - 1)(n + 2)(n^2 + n - 3r^2),$$

$$\beta_5 = 9rs(n-1)(n+2)(2n-1)(2n+3),$$

$$\beta_7 = -35rn(n+1)(3n^2 + 3n - 5r^2 - 1),$$

$$\beta_8 = -45s(n-1)(n+2)(n^2 + n - 3r^2)$$

and

$$\varpi = (n-1)(n+2)(2n-1)(2n+3)n^2(n+1)^2(2n+1)^2.$$

By replacing *r* by s and *s* by *r*, we can get β_3 from β_2, β_6 from β_4, β_9 from β_8 and β_{10} from β_7. So by least squares method the bivariate polynomial (2) is the unique polynomial to fit the data points in three dimensional space.

Evaluating the polynomial (1) at particular points $(\frac{1}{4}, \frac{1}{4}), (\frac{1}{4}, \frac{3}{4}), (\frac{3}{4}, \frac{1}{4}), (\frac{3}{4}, \frac{3}{4}),$ changing the following notations:

$$f_{r,s} = f_i^k + {}_{r,j} + {}_s,$$

$$f(\frac{1}{4},\frac{1}{4}) = f^{k+1}_{2i-1,2j-1,} \qquad f(\frac{1}{4},\frac{3}{4}) = f^{k+1}_{2i,2j-1,}$$
$$f(\frac{3}{4},\frac{1}{4}) = f^{k+1}_{2i-1,2j,} \qquad f(\frac{3}{4},\frac{3}{4}) = f^{k+1}_{2i,2j,}$$

and then by substituting the values of $\beta_1, \ldots, \beta_9, \beta_{10}$, in equation (1), we get $(2n+1)^2$-point approximating subdivision scheme with following four rules to fit a surface to the set of data points at rectangular grid/mesh.

$$f^{k+1}_{2i-1,2j-1} = \frac{1}{\sigma}\sum_{r=-n}^{n}\Big(\sum_{s=-n}^{n}(X^1{}_{r,s} + X^2{}_{r,s})\Big) f^{k}_{i+r,j+s,} \tag{2}$$

where

$$\begin{aligned} X^1_{r,s} = &-\frac{135}{32}rs^2 - \frac{135}{32}r^2s + \frac{27}{8}rs - \frac{45}{8}ns^2 - \frac{1305}{64}n^2s + \frac{525}{64}ns + \frac{735}{64}ns^3 - \frac{945}{64}n^2s^3 - \frac{555}{16}n^3s \\ &-\frac{105}{2}n^4s^3 + \frac{1245}{32}n^4s + \frac{135}{2}n^5s + \frac{45}{2}n^6s - \frac{105}{4}n^4s^3 + \frac{735}{64}nr^3 - \frac{945}{64}n^2r^3 + \frac{135}{2}n^5r \\ &-\frac{105}{2}n^3r^3 + \frac{435}{16}n^2s^2 + \frac{45}{2}n^6r - \frac{105}{4}n^4r^3 + \frac{405}{8}n^3s^2 - 15n^6r^2 - 15n^6s^2 - 45n^5r^2 - 45n^5s^2, \end{aligned}$$

and

$$\begin{aligned} X^2_{r,s} = &-\frac{195}{16}n^4s^2 - \frac{99}{16}nrs + \frac{9}{4}n^4rs + \frac{9}{2}n^3rs - \frac{63}{16}n^2rs + 56n^7 + 14n^8 + \frac{435}{16}n^2r^2 + \frac{1245}{32}n^4r \\ &-\frac{195}{16}n^4r^2 - \frac{555}{16}n^3r - \frac{1305}{64}n^2r + \frac{405}{8}n^3r^2 + \frac{525}{64}nr - \frac{45}{8}nr^2 - \frac{341}{8}n^5 + \frac{409}{8}n^6 - \frac{107}{8}n^3 \\ &+\frac{39}{4}n^2 - \frac{599}{8}n^4 + \frac{1575}{64}nr^2s + \frac{855}{64}n^2r^2s - \frac{45}{4}n^4rs^2 + \frac{1575}{64}nrs^2 + \frac{855}{64}n^2rs^2 - \frac{45}{4}n^4r^2s \\ &-\frac{45}{2}n^3rs^2 - \frac{45}{2}n^3r^2s, \end{aligned}$$

$$f^{k+1}_{2i,2j-1} = \frac{1}{\sigma}\sum_{r=-n}^{n}\Big(\sum_{s=-n}^{n}(X^3_{r,s} + X^4_{r,s})\Big) f^{k}_{i+r,j+s}, \tag{3}$$

where

$$\begin{aligned} X^3_{r,s} = &-\frac{1215}{32}rs^2 - \frac{405}{32}r^2s + \frac{81}{8}rs - \frac{405}{8}ns^2 - \frac{5595}{64}n^2s + \frac{2415}{64}ns + \frac{6405}{64}ns^3 + \frac{1365}{64}n^2s^3 \\ &-\frac{2925}{16}n^3s - \frac{315}{2}n^3s^3 + \frac{2475}{32}n^4s + \frac{405}{2}n^5s + \frac{135}{2}n^6s - \frac{315}{4}n^4s^3 + \frac{735}{64}nr^3 \frac{945}{64}n^2r^3 \\ &+\frac{135}{2}n^5r - \frac{105}{2}n^3r^3 + \frac{75}{16}n^2s^2 + \frac{45}{2}n^6r - \frac{105}{4}n^4r^3 + \frac{765}{8}n^3s^2 - 15n^6r^2 - 15n^6s^2 \\ &-45n^5r^2 - 45n^5s^2 + \frac{165}{16}n^4s^2 - \frac{297}{16}nrs, \end{aligned}$$

and

$$X_{r,s}^{4} = \frac{27}{4}n^4rs + \frac{27}{2}n^3rs - \frac{189}{16}n^2rs + 56n^7 + 14n^8 + \frac{435}{16}n^2r^2 + \frac{1065}{32}n^4r - \frac{195}{16}n^4r^2 - \frac{735}{16}n^3r - \frac{945}{64}n^2r + \frac{405}{8}n^3r^2 + \frac{1245}{64}nr - \frac{45}{8}nr^2 - \frac{521}{8}n^5 + \frac{349}{8}n^6 + \frac{73}{8}n^3 + \frac{99}{4}n^2 - \frac{659}{8}n^4 + \frac{4725}{64}nr^2s + \frac{2565}{64}n^2r^2s - \frac{45}{4}n^4rs^2 + \frac{2655}{64}nrs^2 - \frac{135}{4}n^4r^2s + \frac{1935}{64}n^2rs^2 - \frac{45}{2}n^3r^2s,$$

$$f_{2i-1,2j}^{k+1} = \frac{1}{\sigma}\left(\sum_{r=-n}^{n}\left(\sum_{s=-n}^{n}\left(X_{r,s}^{5} + X_{r,s}^{6}\right)\right) f_{i+r,j+s}^{k}\right), \tag{4}$$

where

$$X_{r,s}^{5} = -\frac{405}{32}rs^2 - \frac{1215}{32}r^2s + \frac{81}{8}rs - \frac{45}{8}ns^2 - \frac{945}{64}n^2s + \frac{1245}{64}ns + \frac{735}{64}ns^3 - \frac{945}{64}n^2s^3 - \frac{735}{16}n^3s - \frac{105}{2}n^3s^3 + \frac{1065}{32}n^4s + \frac{135}{2}n^5s + \frac{45}{2}n^6s - \frac{105}{4}n^4s^3 + \frac{6405}{64}nr^3 + \frac{1365}{64}n^2r^3 + \frac{405}{2}n^5r - \frac{315}{2}n^3r^3 + \frac{435}{16}n^2s^2 + \frac{135}{2}n^6r - \frac{315}{4}n^4r^3 + \frac{405}{8}n^3s^2 - 15n^6r^2 - 15n^6s^2 - 45n^5r^2 - 45n^5s^2 - \frac{195}{16}n^4s^2 - \frac{297}{16}nrs,$$

and

$$X_{r,s}^{6} = \frac{27}{4}n^4rs + \frac{27}{2}n^3rs - \frac{189}{16}n^2rs + 56n^7 + 14n^8 + \frac{75}{16}n^2r^2 + \frac{2475}{32}n^4r + \frac{165}{16}n^4r^2 - \frac{2925}{16}n^3r - \frac{5595}{64}n^2r + \frac{765}{8}n^3r^2 + \frac{2415}{64}nr - \frac{405}{8}nr^2 - \frac{521}{8}n^5 + \frac{349}{8}n^6 + \frac{73}{8}n^3 + \frac{99}{4}n^2 - \frac{659}{8}n^4 + \frac{2655}{64}nr^2s + \frac{1935}{64}n^2r^2s - \frac{135}{4}n^4rs^2 + \frac{4725}{64}nrs^2 + \frac{2565}{64}n^2rs^2 - \frac{45}{4}n^4r^2s - \frac{135}{2}n^3rs^2 - \frac{45}{2}n^3r^2s,$$

$$f_{2i,2j}^{k+1} = \frac{1}{\sigma}\sum_{r=-n}^{n}\left(\sum_{s=-n}^{n}\left(X_{r,s}^{7} + X_{r,s}^{8}\right)\right) f_{i+r,j+s}^{k}, \tag{5}$$

where

$$X_{r,s}^{7} = -\frac{3645}{32}rs^2 - \frac{3645}{32}r^2s + \frac{243}{8}rs - \frac{405}{8}ns^2 - \frac{4515}{64}n^2s + \frac{4575}{64}ns + \frac{6405}{64}ns^3 + \frac{1365}{64}n^2s^3$$
$$-\frac{3465}{16}n^3s - \frac{315}{2}n^3s^3 + \frac{1935}{32}n^4s + \frac{405}{2}n^5s + \frac{135}{2}n^6s - \frac{315}{4}n^4s^3 + \frac{6405}{64}nr^3 + \frac{1365}{64}n^2r^3$$
$$+\frac{405}{2}n^5r - \frac{315}{2}n^3r^3 + \frac{75}{16}n^2s^2 + \frac{135}{2}n^6r - \frac{315}{4}n^4r^3 + \frac{765}{8}n^3s^2 - 15n^6r^2 - 15n^6s^2$$
$$-45n^5r^2 - 45n^5s^2 + \frac{165}{16}n^4s^2 - \frac{891}{16}nrs,$$

and

$$X_{r,s}^{8} = \frac{81}{4}n^4rs + \frac{81}{2}n^3rs - \frac{567}{16}n^2rs + 56n^7 + 14n^8 + \frac{75}{16}n^2r^2 + \frac{1935}{32}n^4r + \frac{165}{16}n^4r^2 - \frac{3465}{16}n^3r$$
$$-\frac{4515}{64}n^2r + \frac{765}{8}n^3r^2 + \frac{4575}{64}nr - \frac{405}{8}nr^2 - \frac{701}{8}n^5 + \frac{289}{8}n^6 + \frac{253}{8}n^3 + \frac{159}{4}n^2 - \frac{719}{8}n^4$$
$$+\frac{7965}{64}nr^2s + \frac{5805}{64}n^2r^2s - \frac{135}{4}n^4rs^2 + \frac{7965}{64}nrs^2 + \frac{5805}{64}n^2rs^2 - \frac{135}{4}n^4r^2s$$
$$-\frac{135}{2}n^3rs^2 - \frac{135}{2}n^3r^2s,$$

where

$\sigma = n^2(n-1)(2n+3)(2n-1)(n+2)(n+1)^2(2n+1)^2$, K represents subdivision level whereas $f_{i,j}^{k+1}$ and $f_{i,j}^{k}$ represent control points (data points) at level $k+1$ and k respectively.

2.1 First refined rule

Figure 2 shows the geometrical arrangement (i.e. stencil) of the coarse points of course mesh to calculate a new point $f_{2i-1,2j-1}^{k+1}$ of refined mesh. The weights a_1 to a_{15} in this figure are

These weights are taken from the rule defined in (2).

$$a_1 = -\frac{733}{22400}, \quad a_2 = -\frac{687}{44800}, \quad a_3 = \frac{1347}{44800},$$
$$a_4 = \frac{1521}{44800}, \quad a_5 = -\frac{41}{560}, \quad a_6 = \frac{3}{128},$$
$$a_7 = \frac{933}{11200}, \quad a_8 = \frac{1061}{11200}, \quad a_9 = -\frac{529}{44800},$$

$$a_{10}=\frac{211}{1400},\quad a_{11}=\frac{1823}{11200},\quad a_{12}=\frac{2237}{44800},$$
$$a_{13}=\frac{151}{896},\quad a_{14}=\frac{1903}{44800},\quad a_{15}=-\frac{2323}{22400}.$$

2.2 Second refined rule

Figure 3 shows the geometrical arrangement of the course points of coarse mesh to calculate a new point $f_{2i,2j-1}^{k+1}$ of refined mesh. The weights b_1 to b_{25} in this figure are

$$b_1=\frac{137}{11200}\ b_2=-\frac{103}{1792}\ b_3=\frac{867}{44800},\ b_4=\frac{2929}{44800}\ b_5=-\frac{2167}{22400}\ b_6=-\frac{113}{8960},$$
$$b_7=-\frac{233}{5600}\ b_8=\frac{793}{11200}\ b_9=\frac{3299}{22400},\ b_{10}=\frac{67}{6400},\ b_{11}=\frac{817}{44800},\ b_{12}=\frac{103}{11200},$$
$$b_{13}=\frac{191}{1400},\ b_{14}=\frac{2493}{11200},\ b_{15}=\frac{4047}{44800},\ b_{16}=\frac{1579}{44800},\ b_{17}=\frac{569}{22400},\ b_{18}=\frac{1643}{11200},$$
$$b_{19}=\frac{621}{2800},\ b_{20}=\frac{657}{8960},\ b_{21}=-\frac{697}{22400},\ b_{22}=-\frac{2801}{44800},\ b_{23}=\frac{1437}{44800},\ b_{24}=\frac{135}{1792},\ b_{25}=-\frac{1233}{11200}.$$

These weights are taken from the rule defined in (3).

2.3 Third refined rule

Figure 4 shows the geometrical arrangement of the course points of coarse mesh to calculate a new point $f_{2i-1,2j}^{k+1}$ of refined mesh. The weights c_1 to c_{25} in this figure are

$$c_1=\frac{137}{11200},\ c_2=-\frac{113}{8960},\ c_3=\frac{817}{44800},\ c_4=\frac{1579}{44800},\ c_5=-\frac{697}{22400},\ c_6=-\frac{103}{1792},$$
$$c_7=-\frac{233}{5600},\ c_8=\frac{103}{11200},\ c_9=\frac{569}{22400},\ c_{10}=-\frac{2801}{44800},\ c_{11}=\frac{867}{44800},\ c_{12}=\frac{793}{11200},$$
$$c_{13}=\frac{191}{1400},\ c_{14}=\frac{1643}{11200},\ c_{15}=\frac{1437}{44800},\ c_{16}=\frac{2929}{44800},\ c_{17}=\frac{3299}{22400},\ c_{18}=\frac{2493}{11200},$$
$$c_{19}=\frac{621}{2800},\ c_{20}=\frac{135}{1792},\ c_{21}=-\frac{2167}{22400},\ c_{22}=\frac{67}{6400},\ c_{23}=\frac{4047}{44800},\ c_{24}=\frac{657}{8960},\ c_{25}=-\frac{1233}{11200}.$$

These weights are taken from the rule defined in (4).

2.4 Fourth refined rule

Figure 5 shows the geometrical arrangement of the course points of coarse mesh to calculate a new point $f_{2i,2j}^{k+1}$ of refined mesh. The weights d_1 to d_{15} in this figure are

$$d_1 = \frac{237}{4480}, \quad d_2 = -\frac{2229}{44800}, \quad d_3 = \frac{657}{44800},$$
$$d_4 = \frac{3083}{44800}, \quad d_5 = -\frac{181}{2800}, \quad d_6 = -\frac{2253}{22400},$$
$$d_7 = \frac{3}{11200}, \quad d_8 = \frac{169}{2240}, \quad d_9 = -\frac{2347}{44800},$$
$$d_{10} = \frac{171}{1400}, \quad d_{11} = \frac{2273}{11200}, \quad d_{12} = \frac{2927}{44800},$$
$$d_{13} = \frac{6137}{22400}, \quad d_{14} = \frac{4981}{44800}, \quad d_{15} = -\frac{59}{640}.$$

These weights are taken from the rule defined in (5).

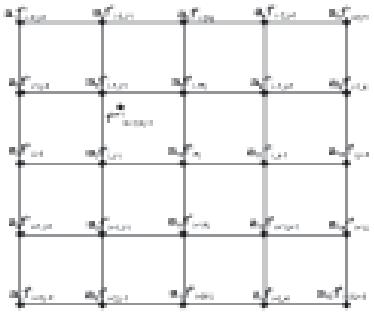

Figure 2. Geometrical arrangement to insert new point $f^{k+1}_{2i-1,2j-1}$ which is shown by solid filled circle. Solid lines show coarse grid/mesh while solid diamonds are coarse points.

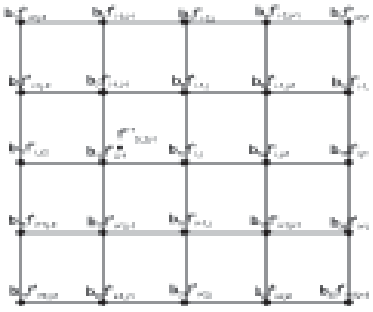

Figure 3. Geometrical arrangement to insert new point $f^{k+1}_{2i,2j-1}$ which is shown by solid filled circle. Solid lines show coarse grid/mesh while solid diamonds are coarse points.

Remark 1. By substituting the different values of n (i.e. $n = 2, 3, 4, \ldots$) in $(2n + 1)^2$-point approximating subdivision scheme, we get different schemes.

2.5 Applications of proposed scheme

Here we present the numerical experiment to check the efficiency and validity of the proposed $(2n + 1)^2$-point approximating subdivision scheme. Figure 6 shows the vertex insertion by subdivision rules $f_{2i-1,2j-1}^{k+1}$, $f_{2i,2j-1}^{k+1}$, $f_{2i-1,2j}^{k+1}$ and $f_{2i,2j}^{k+1}$.

Figure 7 shows the course mesh with refined mesh and Figure 8 shows the refined mesh only. Figure 9 (a) shows the initial mesh by which the subdivision process will goes on, Figure 9 (b)-(c) shows the subdivision at first and second

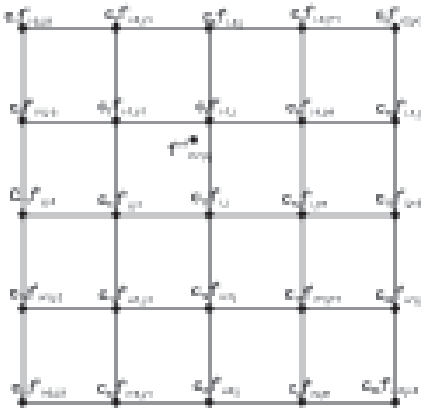

Figure 4. Geometrical arrangement to insert new point $f_{2i-1,2j}^{k+1}$ which is shown by solid filled circle. Solid lines show coarse grid/mesh while solid diamonds are coarse points.

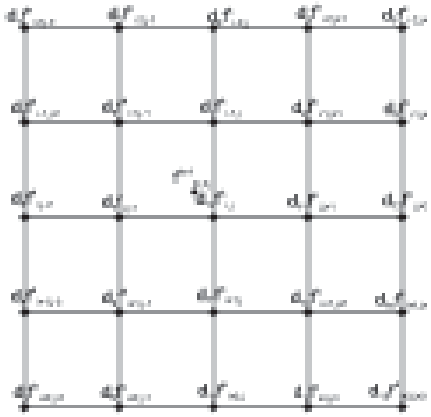

Figure 5. Geometrical arrangement to insert new point $f_{2i,2j}^{k+1}$ which is shown by solid filled circle. Solid lines show coarse grid/mesh while solid diamonds are coarse points.

level respectively by the proposed scheme for $n = 2$. Finally Figure 9 (d) shows the limit surface generated by successive refinement steps.

3. Conclusion

We have generated $(2n + 1)^2$-point approximating subdivision scheme for surface modeling by fitted the bivariate cubic polynomial to the data with the help of least squares method. The rules for implementations of the schemes are clearly described. The visual smoothness of the proposed schemes are presented by different refinement levels.

In future, we can extend the proposed work from regular topology to arbitrary topology which will be more useful in many engineering applications.

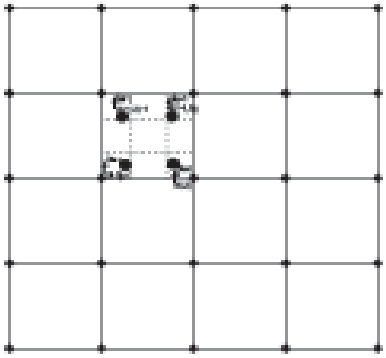

Figure 6. Shows the insertion of vertices by using the refinement rules

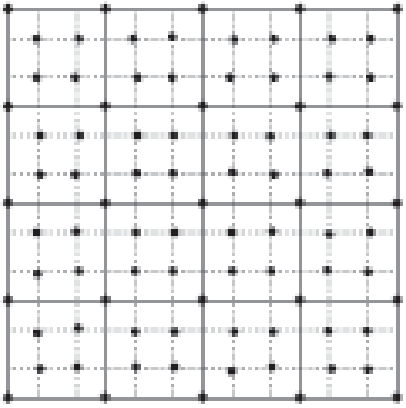

Figure 7. Shows the course mesh with refined mesh

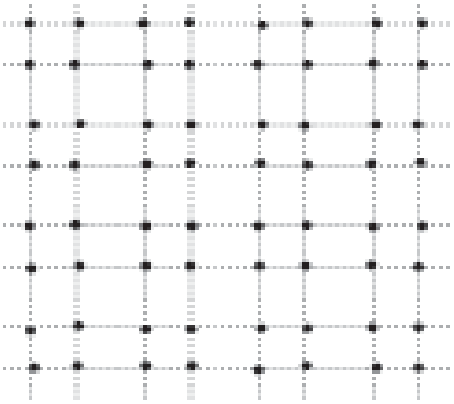

Figure 8. Shows the refined mesh only

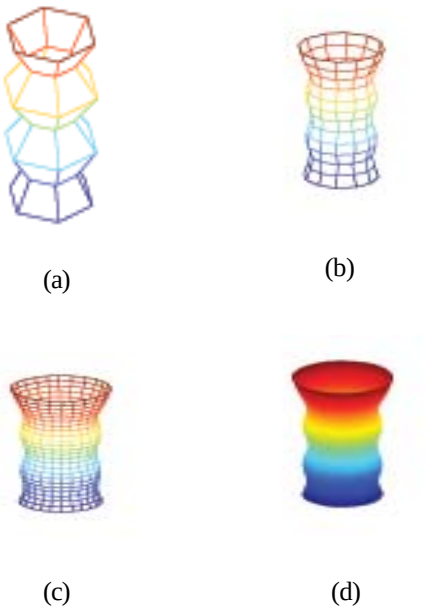

(a) (b)

(c) (d)

Figure 9. (a)-(d) show the initial mesh, first level, second level and limit curve respectively

Acknowledgement

This work is supported by NRPU Project No. 3183 ofHigher Education Commission, Pakistan.

References

[1] Kopka, H., Daly, P. W. (1999). A Guide to LATEX, 3rd ed. Harlow, England: Addison-Wesley.

[2] Chaikin, G. M. (1974). An algorithm for high-speed curve generation. *Computer Graphics and Image Processing*. 3. 346-349.

[3] Doo, D., Sabin, M. (1978). Behaviour of recursive division surfaces near extraordinary points. *Computer-Aided Design*. 10. 356-360.

[4] Conti, C., Romani, L (2013). Dual univariate m-ary subdivision scheme of de Rham-type. *Journal of Mathematics Analysis and Applications*. 407. 443- 456.

[5] Antonelli, M., Beccari, C. V., Casciola, G. Ciarloni, R. , Morigi, S (2013). Subdivision surfaces integrated in a CAD system. *Computer-Aided Design*. 45. 1294-1305.

[6] Kosinka, J., Sabin M Dodgson, N.(2013) Cubic subdivision schemes with double knots. *Computer Aided Geometric Design*. 30. 45-57.

[7] Beccari, C. V. Casciola G. Romani, L. (2013). Non-uniform non-tensor product local interpolatory subdivision surfaces. *Computer Aided Geometric Design*. 30. 357-373.

[8] Deng C. Lin, H. (2014). Progressive and iterative approximation for least squares B-spline curve and surface fitting. *Computer-Aided Design*. 47. 32-44.

[9] Shi B-Q. Liang, J. (2016). An integration method for scanned multi-view range image (MRIs) based on local weighted least squares (LWLS) surface fitting. Optics and Lasers in Engineering. 77. 64-78.

[10] Vilca, F. Romeiro , R. G. Balakrishnan, N (2016). A bivariate Birnbaum-Saunders regression model. Computational Statistics and Data Analysis. 97. 169-183.

[11] Dyn, N.Heard, A., Hormann K Sharon, N. (2015) Univariate subdivision scheme for noisy data with geometric applications. *Computer Aided Geometric Design*. 37. 85-104.

[12] Mustafa, G., Li, H.,Zhang, J. , Deng, J (2015). *l*1-Regression based subdivision schemes for noisy data. *Computer-Aided Design.* 58. 189-199.